Multifunctionalized iron oxide nanoparticles for selective drug delivery to CD44-positive cancer cells

# Multifunctionalized iron oxide nanoparticles for selective drug delivery to CD44-positive cancer cells

**Antonio Aires**[1,2], **Sandra M Ocampo**[1], **Bruno M Simões**[3],
**María Josefa Rodríguez**[1,4], **Jael F Cadenas**[1], **Pierre Couleaud**[1,2],
**Katherine Spence**[3], **Alfonso Latorre**[1,2], **Rodolfo Miranda**[1],
**Álvaro Somoza**[1,2], **Robert B Clarke**[3], **José L Carrascosa**[1,4] **and**
**Aitziber L Cortajarena**[1,2]

[1] Instituto Madrileño de Estudios Avanzados en Nanociencia (IMDEA Nanociencia), Campus de Cantoblanco, 28049 Madrid, Spain
[2] CNB-CSIC-IMDEA Nanociencia Associated Unit, Cantoblanco, Madrid, Spain
[3] Breast Biology, Breakthrough Breast Cancer Research Unit, Institute of Cancer Sciences, University of Manchester, Paterson Building, Wilmslow Road, Manchester M20 4BX, UK
[4] Department of Structure of Macromolecules, Centro Nacional de Biotecnología/CSIC, Cantoblanco, Madrid, Spain

E-mail: aitziber.lopezcortajarena@imdea.org

## Abstract
Nanomedicine nowadays offers novel solutions in cancer therapy and diagnosis by introducing multimodal treatments and imaging tools in one single formulation. Nanoparticles acting as nanocarriers change the solubility, biodistribution and efficiency of therapeutic molecules, reducing their side effects. In order to successfully apply these novel therapeutic approaches, efforts are focused on the biological functionalization of the nanoparticles to improve the selectivity towards cancer cells. In this work, we present the synthesis and characterization of novel multifunctionalized iron oxide magnetic nanoparticles (MNPs) with antiCD44 antibody and gemcitabine derivatives, and their application for the selective treatment of CD44-positive cancer cells. The lymphocyte homing receptor CD44 is overexpressed in a large variety of cancer cells, but also in cancer stem cells (CSCs) and circulating tumor cells (CTCs). Therefore, targeting CD44-overexpressing cells is a challenging and promising anticancer strategy. Firstly, we demonstrate the targeting of antiCD44 functionalized MNPs to different CD44-positive cancer cell lines using a CD44-negative non-tumorigenic cell line as a control, and verify the specificity by ultrastructural characterization and downregulation of CD44 expression. Finally, we show the selective drug delivery potential of the MNPs by the killing of CD44-positive cancer cells using a CD44-negative non-tumorigenic cell line as a control. In conclusion, the proposed multifunctionalized MNPs represent an excellent biocompatible nanoplatform for selective CD44-positive cancer therapy *in vitro*.

[S] Online supplementary data available from stacks.iop.org/NANO/27/065103/mmedia

(Some figures may appear in colour only in the online journal)

# 1. Introduction

The use of nanoparticles for drug delivery in cancer treatment is a widely studied scientific field and is continuously progressing [1]. Smart design of the nanocarriers allows their use for drug delivery, presenting several advantages such as an improvement in drug solubility, the intracellular accumulation of the chemotherapeutics transported, a longer lifetime in the bloodstream, and a decrease in the multidrug resistance [2–5]. Drug delivery using a wide variety of nanoparticles has been intensively studied in the last 20 years [6–8]. In particular, MNPs offer an extra therapeutic mode associated with the hyperthermia generated after magnetic activation [9], and an additional diagnostic advantage, as contrast agents in magnetic resonance imaging (MRI) techniques [10, 11].

In spite of recent advances in nanotechnology-based therapies, controlling the targeting of specific cells (i.e. cancer cells or cancer stem cells) still remains a challenge. This specificity would increase the treatment efficiency and also avoid secondary effects. CD44 is a multifunctional cell surface protein involved in proliferation and differentiation, angiogenesis and signalling [12]. It has been reported that CD44 is overexpressed in a large number of cancer cells but also in CSCs [13, 14], and CTCs [15–17]. Among several surface receptors overexpressed in CSCs, including CD133, CD44, CD49 and ITGA6, CD44 is the most frequent molecular marker, being present in a large variety of tumor types [18]. Indeed, the most commonly used breast CSC phenotype is the $CD44^+CD24^{-/low}$ phenotype defined for the first time in 2003 [19] and breast tumours positive for the stem cell marker CD44 have been shown to have decreased patient survival [20]. Considering that treating CSCs [21] and CTCs [15] is fundamental for a complete elimination of tumour tissue, targeting CD44-expressing cells is a challenging and promising anticancer strategy [12].

A diversity of nanomaterials including natural polymers, carbon nanotubes, lipid-based, and inorganic nanoparticles have been proposed for the specific targeting CD44-expressing cells. Most of them have been formulated by the conjugation of a given nanovehicle with hyaluronic acid (HA) [22], but in general, preliminary results have not been so promising [18, 23, 24]. In this regard, the use of antibodies against specific membrane markers of cancer cells is a promising targeting strategy due to the high affinity for their corresponding antigen [25]. As it has been postulated by Paul Ehrlich at the very beginning of the 20th century, and recently discussed [26], the use of antibodies as a so called 'Magic Bullet', should permit 'drugs to go straight to their intended cell-structural targets'.

In this study, we demonstrate the specific targeting and the selective drug delivery to different CD44-positive cancer cell lines (Panc-1[27, 28] and MDA-MB-231[29, 30]) representative of pancreatic and breast cancers, in which CD44 is an extensively used surface marker. To better demonstrate the specific targeting of CD44-positive cancer cells we have used a non-tumorigenic breast cell line as negative control. The targeting of specific tumour cells is achieved by the CD44 antibody, which is attached onto the

MNP surface covalently and correctly oriented. On the other hand, the cytotoxic effect is ensured by the chemotherapeutic gemcitabine (GEM) that is currently used for pancreatic cancer treatment in clinic. The linker used for the covalent immobilization of gemcitabine has been designed to perform the release of the drug only in an intracellular environment, contributing to the selectivity of this drug delivery system [31]. What is more, MNPs such as the ones used in this study, have two advantages compared with other nanoplatforms as they can also be used to kill cancer cells through hyperthermia and act as contrast agents in MRI [32]. Those two advantages are not discussed in the present study but have to be taken into account for further *in vivo* studies with the nanostructures developed here.

# 2. Materials and methods

## 2.1. Materials

Purified mouse antihuman CD44 antibodies (Cat: 555478) were purchased from BD PharmigenTM. Gemcitabine was purchased from Fluorochem. Ultrapure reagent grade water (18.2 M$\Omega$, Wasserlab) was used in all experiments. Dimercaptosuccinic acid (DMSA) coated MNPs (zeta potential: $-59$ mV, hydrodynamic diameter (Z-average): 59 nm (PDI:0.22) and TEM are shown in supporting information, figures S1 and S2A, available at stacks.iop.org/NANO/27/065103/mmedia) have been provided by Dr Gorka Salas' group from IMDEA Nanociencia and prepared as previously described [11]. Gemcitabine derivative, GEM-S-S-Pyr was prepared according to described procedures [31].

## 2.2. Cell culture

Panc-1, MDA-MB231 and MCF-10A cell lines were purchased from American Type Culture Collections (Manassas, VA, USA). Panc-1 and MDA-MB231 cell lines were grown as monolayer in Dulbecco's Modified Eagle's Medium (DMEM) supplemented with 10% fetal bovine serum (FBS), 2 mM L-glutamine, 0.25 $\mu$g ml$^{-1}$ fungizone, 100 units of penicillin per ml and 100 $\mu$g ml$^{-1}$ of streptomycin. MCF-10A was grown as monolayers in human uterine microvascular endothelial cells (HuMEC) ready medium from GIBCO (HuMEC basal serum-free medium supplemented with epidermal growth factor, hydrocortisone, isoproterenol, transferrin, insulin and 25 mg of bovine pituitary extract) supplemented with 100 units of penicillin and 100 mg ml$^{-1}$ of streptomycin (Lonza). All reagents were purchased from GIBCO. Cell lines were maintained in an incubator at 37 °C in a humidified atmosphere of 95% air and 5% $CO_2$.

## 2.3. Measurements

Ultraviolet-visible (UV-Vis) and fluorescence spectra were recorded on a Synergy H4 microplate reader (BioTek) using 96-well plates. Hydrodynamic diameter and zeta potential measurements were determined using a Zetasizer Nano-ZS device (Malvern Instruments). Hydrodynamic diameter and

zeta potential were measured from dilute sample suspensions (0.1 mg Fe per ml) in water at pH 7.4 using a zeta potential cell. High-performance liquid chromatography (HPLC) was performed using a 1260 Infinity HPLC (Agilent Technologies) with a ZORBAX 300SB-C18 column 5 $\mu$m, 9.4 $\times$ 250 mm.

### 2.4. MNP sterilization

We always carried out the MNP sterilization before cell incubation. 500 $\mu$l of MNP stock was dispersed by sonication for 5 min and then the MNPs were mixed with medium containing 10% FBS until desired concentration. The resulting sample was filtered through a 0.22 $\mu$m Millex-GP filter (Merck-Millipore Darmstadt, Germany) and sonicated again for 1 min.

### 2.5. Multifunctionalization of DMSA MNPs

#### 2.5.1. Pre-activation of MNPs.
5 ml of MNPs at 2.4 mg Fe per ml were incubated overnight at room temperature with 50 $\mu$mol of cysteamine hydrochloride per g Fe, previously neutralized by 1 molar equivalent of sodium hydroxide (NaOH), 150 $\mu$mol of 1-Ethyl-3-(3-dimethylaminopropyl) carbodiimide (EDC) per gram of Fe and 75 $\mu$mol of n-hydroxysuccinimide (NHS) per gram of Fe. After 16 h, the sample was washed by cycles of centrifugation and redispersion in Milli-Q water 3 times. The presence of sulfhydryl groups introduced onto the MNPs was quantitatively measured by reaction with 2, 4-dinitrothiocyanatebenzene (DNTB) [33].

#### 2.5.2. Covalent immobilization of antiCD44 antibodies on MNPs.
A solution of the CD44 antibodies (1 mg ml$^{-1}$) in 0.01 M 4-(2-hydroxyethyl)-1-piperazineethanesulfonic acid (HEPES), 0.15 M sodium chloride (NaCl), pH 8.2, was incubated for 1 hour at room temperature with a 40 molar equivalents solution of 2-iminothiolane (Traut's reagent). After that, the modified antibody was purified by gel filtration through a desalting resin (Sephadex G-25) using 0.1 M sodium phosphate, 0.15 M NaCl, pH 7.4. The sulfhydryl groups of MNP were activated as follows: 2 ml of aqueous suspension of pre-activated MNP at 2.4 mg Fe per ml was mixed with 24 $\mu$l of 2-aldrithiol solution at 5 mM in dimethyl sulfoxide (DMSO) (0.12 $\mu$mol, 25 $\mu$mol per g Fe) during 2 h at 40 °C. After reaction, 200 $\mu$l of brine were added and the sample centrifuged 10 min at 10 000xg and redispersed in 2 ml of 0.01 M sodium phosphate, pH 7.4 and incubated at 4 °C overnight with 200 $\mu$l of modified antiCD44 antibody solution at 840 $\mu$g ml$^{-1}$ in 0.1 M sodium phosphate, 0.15 M NaCl, pH 7.4. After that, the MNP-antiCD44 was purified by gel filtration through a sepharose CL-6B column using 0.01 M sodium phosphate buffer, pH 7.4. The remaining sulfhydryl activated groups were blocked at 25 °C for 1 h with 24 $\mu$l of 3-mercaptopropionic acid solution at 4 mM in 0.01 M sodium phosphate, pH 7.4 (0.096 $\mu$mol, 20 $\mu$mol per g Fe). Finally, MNP were washed several times with 0.01 M sodium phosphate, pH 7.4 and stored at 4 °C until used.

Samples of supernatants before and after the immobilization process were withdrawn and measured using Bradford assay [34]. A reference solution was prepared with exactly the initial antibody concentration and media conditions (pH, ionic strength) and bovine serum albumin (BSA) was used as protein standard. The amount of bound antibodies was determined from the difference between the not conjugated antibody concentration in the supernatant and the initial antibody (Ab) concentration ($\mu$g Ab per mg Fe).

#### 2.5.3. Covalent immobilization of GEM and antiCD44 antibodies on MNPs.
First, a GEM derivative (0.36 $\mu$mol, 30 $\mu$mol per g Fe) was added to react with sulfhydryl pre-activated MNPs (5 ml at 2.4 mg Fe per ml). The covalently immobilized GEM was determined by quantification of the 2-pyridinethione released during the reaction ($\lambda_{max} = 343$ nm, $\varepsilon_{343nm} = 8080$ M cm$^{-1}$). Then the remaining sulfhydryl groups of MNP-GEM were activated as follows: 5 ml of aqueous suspension of sulfhydryl activated MNP-GEM at 2.4 mg Fe ml$^{-1}$ was mixed with 60 $\mu$l of 2-aldrithiol solution at 5 mM in DMSO (0.3 $\mu$mol, 25 $\mu$mol per g Fe) for 2 h at 40 °C. After reaction, 200 $\mu$l of brine were added and the sample centrifuged 10 min at 10 000xg and redispersed in 5 ml of 0.01 M sodium phosphate, pH 7.4. Finally, the antiCD44 antibodies were immobilized on MNP-GEM following the same protocol described above for immobilization on MNP.

#### 2.5.4. Drug release studies.
The cumulative drug releases from the MNP-GEM and MNP-GEM-antiCD44 were carried out under physiological conditions (pH 7.4 and 37 °C) using two different concentrations of glutathione (GSH) as the reducing agent (1 $\mu$M and 1 mM of GSH to mimic the extracellular and intracellular conditions, respectively). For each experiment, 4.8 mg of MNP-GEM and MNP-GEM-antiCD44 were dissolved in 1 ml of 0.01 M phosphate buffer at pH 7.4 containing either 1 $\mu$M of GSH or 1 mM GSH and incubated at 37 °C. The amount of GEM released was analysed at regular time intervals by HPLC using a C18 column, mobile phase water/acetonitrile 80/20, at flow rate of 0.3 ml min$^{-1}$, the absorbance was measured at 270 nm. The percentage of GEM released was calculated from a standard calibration curve of the free-drug solution.

### 2.6. In vitro studies

#### 2.6.1. Targeting cancer cells with MNP-antiCD44.
To determine the specific targeting of MNP-antiCD44 for CD44-positive cancer cell lines (Panc-1 and MDA-MB231) in comparison with a non-tumorigenic cell line (MCF-10A), cells were seeded at 2.5 $\times$ 10$^4$ cells per well in 500 $\mu$l of DMEM containing 10% FBS or HuMEC ready medium. After 24 h, the growth medium was removed and cells were then incubated for 4 h at 4 °C in the presence of MNP and MNP-antiCD44 (0.2 mg Fe per ml, Ab 30 $\mu$g per mg Fe, 4 $\mu$M GEM). After incubation, cells were washed three times with phosphate-buffered saline (PBS). Prussian blue staining of iron, processing for electron microscopy and inductively

coupled plasma mass spectrometry (ICP-MS) were performed to investigate the specific binding of MNP-antiCD44 to cells expressing CD44 receptor.

*2.6.2. Prussian blue staining.* For Prussian blue staining, cells were seeded on 12 mm square glass coverslips (Maienfeld GmbH & Co.KG, Germany) placed into the wells. Briefly, the cells were washed twice with phosphate-buffered saline (PBS) (AMRESCO, Ohio, USA) and fixed with 4% paraformaldehyde solution for 30 min at room temperature. The cells were then washed twice with PBS again, and subsequently incubated with a 1:1 mixture of 4% potassium ferrocyanide and 4% hydrochloric acid (Prussian blue staining solution) for 15 min at room temperature before being washed with distilled water three times. The counterstaining was done for cytoplasm with neutral red 0.5% (Panreac Química S.L.U) for 2 min at room temperature and then washed with distilled water several times. After drying the cells, a cover slip was mounted by using DePeX (SERVA Electrophoresis GmbH) and finally the cells were observed using light microscopy (Leica DMI3000B, Leica Microsystems, Germany). All experiments were carried out in triplicate.

*2.6.3. ICP-MS.* For ICP-MS, the cells were washed twice with PBS (AMRESCO, Ohio, USA), trypsinized with 200 $\mu$l of 0.25% w/v trypsin solution and were then incubated for 5 min at 37 °C. When a single cell suspension was obtained, 2 ml of complete media was added. The resultant solution was transferred to a sterile 15 ml conical centrifuge tube and spun down at 1200 rpm for 10 min. The supernatant was discarded carefully and cells were resuspended in 5 ml of fresh complete media and 100 $\mu$l was retained to count the cell number. The cell suspension was centrifuged again at 1200 rpm for 10 min and the supernatant was discarded carefully. 300 $\mu$l of 37% HCl was added to the cell pellet and the resultant suspension was sonicated for 30 min at 40 °C. Finally, 2700 $\mu$l of bi-distilled water was added and the iron concentration was determined by measuring the sample in an ICP-MS NexION 300XX (Perkin Elmer).

*2.6.4. Electron microscopy.* For ultrastructural studies, MDA-MB-231 cells (both control and with nanoparticles) were adhered to coverslips, fixed in 2% formaldehyde and 2.5% glutaraldehyde for 1 h and then processed for embedding in the epoxy resin EML-812 (TAAB laboratories, Berkshire, UK) as previously described [35]. After washing with PBS and water, post-fixation of cells was done with 1% osmium tetroxide in PBS for 45 min. After extensive washing with water, samples were treated with 1% uranyl acetate in water for 45 min, washed again and dehydrated in increasing concentrations of ethanol (50, 75, 95 and 100%, 15 to 30 min each one). After 1 h of incubation with a 1:1 mixture of ethanol and epoxy resin 812, cells were infiltrated with pure epoxy resin 812 at room temperature overnight. The polymerization of infiltrated samples was done in capsules for 2 days at 60 °C. Resin was detached from the coverslips by successive immersions in liquid nitrogen and hot water. Ultrathin sections (70 nm thick) were obtained using a Leica EM UC6 ultramicrotome and a 35° diamond knife (Diatome), transferred to formvar-coated EM buttonhole grids and stained with saturated uranyl acetate for 10 min and lead citrate for 3 min. Sections were visualized on a JEOL JEM 1011 electron microscope operating at 100 kV and equipped with a CCD camera.

*2.6.5. Downregulation of CD44 expression by siRNA.* For specific knockdown of CD44, a mixture of four CD44 small interfering ribonucleic acid (siRNA) was used: SMARTpool ON-TARGET plus Human CD44 siRNA (Cat No: L-009999-00-0005, Dharmacon). ON-TARGET plus Non-targeting pool (Cat No: D-001810-10-05, Dharmacon) was used as a control. MDA-MB-231 cells seeded in Millicell EZ slides (PEZGS0416, Millipore) at $5 \times 10^4$ cells per well were transfected after 24 h with either siRNA against CD44 or control siRNA at a final concentration of 5 nM. Cells were transfected using DharmaFECT 1 Transfection Reagent (Cat No: T-2001-01, Dharmacon) following the manufacturer's instructions. Cells were then incubated at 37 °C in 5% $CO_2$ for 72 h before adding MNPs for 4 h at 4 °C as described in 2.6.1. Cells were then washed three times with PBS and incubated for further 24 h at 37 °C in 5% $CO_2$. Prussian blue staining was performed to confirm specific binding and internalization of MNP-antiCD44 to cells expressing CD44.

## 2.7. In vitro cytotoxicity assays

Resazurin dye (Sigma-Aldrich) has been broadly used as a reliable indicator of cell viability in proliferation and cyto-toxicity assays. To assess cell death, cells (Panc-1, MDA-MB231 and MCF-10A) were cultured on a 24-well plate at a density of $2.5 \times 10^4$ cells per well in 500 $\mu$l of DMEM containing 10% FBS or HuMEC ready medium. After 24 h, the growth medium was removed and cells were then incubated 4 h at 4 °C in the presence of different concentrations of free GEM (4, 1 and 0.4 $\mu$M), MNP-GEM and MNP-GEM-antiCD44 (0.2 mg Fe per ml, 4 $\mu$M GEM). After incubation, cells were washed three times with PBS and then maintained in of DMEM containing 10% FBS or HuMEC ready medium at 37 °C and 5% $CO_2$ incubator. After 72 h, the medium was replaced with of DMEM containing 10% FBS or HuMEC ready medium, and 10% of Resazurin dye (1 mg per ml PBS). Cells were maintained at 37 °C and 5% $CO_2$ incubator for 3 h and then, a Synergy H4 microplate reader was used to determine the amount of Resazurin by measuring the absorbance of the reaction mixture (excitation 570 nm, emission 600 nm). 600 $\mu$l of 10% of resazurin dye was added to empty wells as a negative control. The viability of the cells was expressed as the percentage of absorption of treated cells in comparison with control cells (without nanoparticles). All experiments were carried out in triplicate. All the data obtained were plotted and statistically analysed using the software package GraphPad Prism version 5.0 for Windows. All samples were compared using a one-way ANOVA and Bonferroni post hoc test (*$P < 0.05$, **$P < 0.01$, and
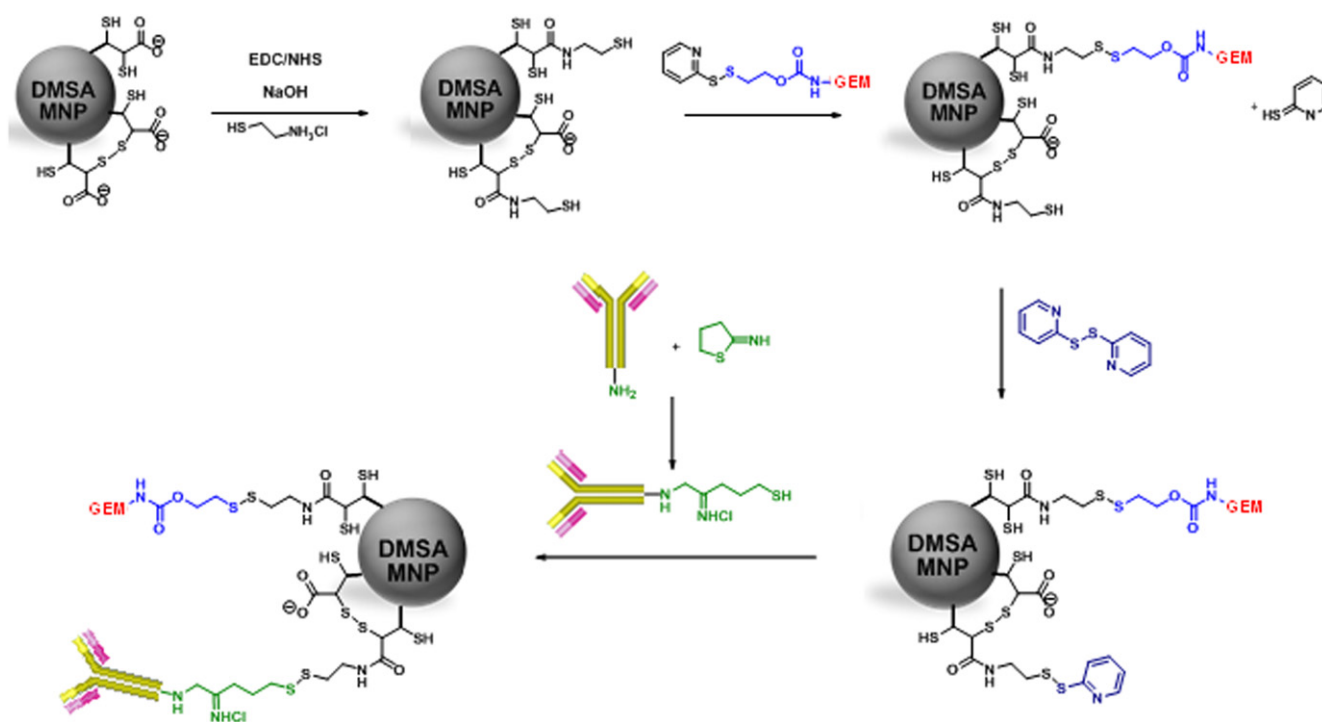
**Figure 1.** General scheme of the multifunctionalization of DMSA MNPs.

***P < 0.001). Only significant differences among the samples are indicated in the charts.

## 3. Results and discussion

This paper describes the potential of functionalized MNPs with antiCD44 antibodies to target CD44-positive cancer cells, and multifunctionalized MNPs with GEM and antiCD44 antibodies to target and kill CD44-positive pancreatic cancer cells. To this end, antiCD44 antibody functionalized MNPs were produced by the formation of disulfide bonds between the reactive thiol of the modified antiCD44 antibody with Traut's reagent and the activated sulfhydryl groups of the pre-modified DMSA MNPs (figure 1). The multifunctionalization strategy through disulfide bonds started with the introduction of a controlled amount of GEM followed by immobilization of the antiCD44 antibodies on MNP-GEM (figure 1).

### 3.1. Multifunctionalization of DMSA MNPs

Disulfide bond-based linkers have been employed for the multifunctionalization of MNPs with targeting agents and drugs. Specifically, we have employed a self-immolative linker that is able to release the chemotherapeutic drugs without any modification. The process is triggered under high reducing conditions, such as the intracellular environment of the tumour cells [31, 36].

As shown in figure 1, the general multifunctionalization strategy starts with the introduction of free thiol functions onto the MNPs. This modification was achieved by the

reaction of cysteamine with the carboxylic groups of the DMSA coating in the presence of EDC and NHS. The process leads to MNPs bearing approximately 30 $\mu$mol of thiols per g Fe (zeta potential of $-50$ mV and hydrodynamic diameter (Z-average) of 63 nm (PDI:0.22)) (DLS histograms are shown in supporting information, figure S2B).

The functionalization of MNPs with antibodies was achieved by the formation of disulfide bonds between the reactive thiol of the modified antiCD44 antibodies and the activated sulfhydryl groups of the MNPs. The introduction of free thiol groups onto the antibodies was performed by the reaction between Traut's reagent and the amine groups of the antibodies [37]. In an antibody molecule, it is possible to distinguish at least two types of amino groups exposed to the medium: (i) the terminal amino groups and (ii) the $\varepsilon$-amino moiety of lysine residues. While terminal amino groups have a pK around 7–8, $\varepsilon$-amino groups of Lys residues have a pK close to 10 [38]. At pH values less than 8.0, the Ab amino terminal groups are the most reactive. As the amino terminal moieties are located in the Fab region where antigen recognition takes place, the Ab modification at this pH condition could contribute to a lower activity of the Ab group after its functionalization. At pH values higher than 8.0, the $\varepsilon$-amino groups of Lys residues are more reactive and as the majority of the lysine residues are located in the Fc portion, the modification should occur preferentially in the Fc portion [38–40]. Therefore, the Ab modification was carried out at pH values higher than 8.0 by employing a 0.01 M HEPES, 0.15 M NaCl, pH 8.2 solution. After the reaction, the immobilized antibodies were quantified by the Bradford assay. The standard load obtained of covalently linked antiCD44 antibodies was 30 mg per g Fe (87%),
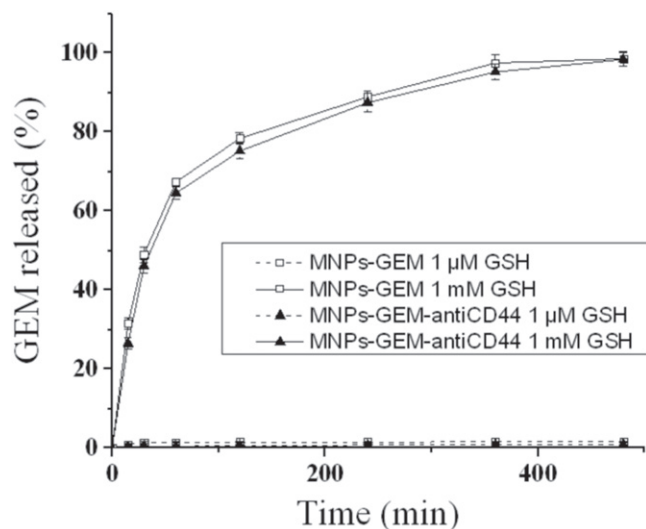
**Figure 2.** Release kinetics of GEM from MNP-GEM (empty squares, 1 mM GSH solid line and 1 $\mu$M GSH dashed line) and MNP-GEM-antiCD44 (filled triangles, 1 mM GSH solid line and 1 $\mu$M GSH dashed line).

corresponding to around one antibody molecule per nanoparticle. The remaining pyridyldisulfide groups were blocked with 3-mercaptopropionic acid. No release of immobilized Ab was observed at this step, due to the higher reactivity of pyridyldisulfide groups. After that, the MNP-antiCD44 was purified by gel filtration through a sepharose CL-6B column using 0.01 M sodium phosphate, pH 7.4 solution. The sodium phosphate MNP-antiCD44 suspension was stable for weeks stored at 4 °C without noticeable precipitation (zeta potential of −44 mV and hydrodynamic diameter (Z-average) of 82 nm (PDI:0.22) (DLS histograms are shown in supporting information, figure S2C).

To obtain multifunctional formulations with antibodies and GEM, firstly the GEM drug derivative was immobilized following a procedure that has been already described[31], leading to a formulation that contains 20 $\mu$mol GEM per g Fe (zeta potential of −49 mV and hydrodynamic diameter (Z-average) of 73 nm (PDI:0.21) (DLS histograms are shown in supporting information, figure S2D). Then, the antiCD44 antibodies were immobilized on MNP-GEM following the same protocol described above for immobilization on MNP. The final formulation contains 20 $\mu$mol GEM and 30 mg Ab per g Fe (zeta potential of −41 mV and hydrodynamic diameter (Z-average) of 93 nm (PDI:0.18) (DLS histograms are shown in supporting information, figure S2E).

### 3.2. Drug release studies

In order to evaluate the potential of MNP-GEM and MNP-GEM-antiCD44 as selective cancer therapy agents, we initially studied their stimuli-response behavior under reducing environment. The drug release was monitored at 37 °C in 0.01 M sodium phosphate, pH 7.4 using 1 $\mu$M or 1 mM of GSH to mimic the extracellular and intracellular conditions, respectively (figure 2). Both formulations showed similar standard release, 96–98% when treated with 1 mM GSH

(mimicking intracellular conditions) after 6–8 h while only 3–5% of the cargo was released with 1 $\mu$M GSH (mimicking the extracellular environment) after 6–8 h (figure 2). These results show that the release of GEM from MNP-GEM and MNP-GEM-antiCD44 is selective and strongly dependent on the reducing environment, so that it will take place mostly inside the cells and is not affected by the presence of the antibody.

### 3.3. Specific targeting of cancer cells with MNP-antiCD44

Specific targeting of cancer cells expressing the CD44 receptor in comparison with a non-tumorigenic CD44-negative cell line was determined by incubating cells for 4 h at 4 °C with MNP-antiCD44 and MNPs (as a negative control), followed by several washes with PBS. The incubation process was done at 4 °C in order to avoid non-specific endocytosis processes and to highlight the specific interactions of antiCD44 with the CD44 receptor. Then, three complementary tests were carried out: specific iron detection, ultrastructural characterization by electron microscopy and analysis of downregulation of CD44 expression.

*3.3.1. Iron staining and ICP-MS.* Prussian blue staining and ICP-MS were used to monitor the presence of iron from the MNP. As shown in figure 3, in the case of MNP without antiCD44, no MNPs were detected by Prussian blue staining. In the case of MNP-antiCD44, a large amount of MNPs was observed surrounding the cell membrane of both CD44-positive cancer cells (Panc-1 and MDA-MB-231) (figures 3(a), (c)) while MNP was not observed surrounding the CD44-negative non-tumorigenic cells (MCF-10A) (figure 3(e)). The results obtained from incubating CD44-positive cancer cells and CD44-negative non-tumorigenic cells with MNP, with and without antiCD44 antibodies, show specific targeting of antiCD44 antibody functionalized MNPs to both cancer cells expressing CD44 receptors. These results were confirmed by ICP-MS ($n = 3$), showing that for MNP-antiCD44, $11.4 \pm 0.6$ pg of Fe per cell was observed in Panc-1 cells and $13.3 \pm 0.3$ pg of Fe per cell in the MDA-MB-231 cells. In the case of MNPs without the antiCD44 antibody, $0.5 \pm 0.1$ pg of Fe per cell was measured in both cancer cell lines.

To demonstrate more effectively the selective targeting of MNP-antiCD44 to CD44-positive cancer cells, ultrastructural characterization by electron microscopy and analysis of downregulation of CD44 expression were done using the MDA-MB-231 breast cancer cell line because this cell line contained higher iron concentrations as anlysed by ICP-MS after MNP-antiCD44 incubation, confirming higher levels of CD44 expression in this cell line than in Panc-1, as has been previously reported [27–30].

*3.3.2. Ultrastructural analysis.* MDA-MB-231 cells incubated with MNPs either with or without antiCD44 were embedded in resin and thin-sectioned for study by transmission electron microscopy. Figure 4(a) shows a characteristic field where the MNPs without the antibody
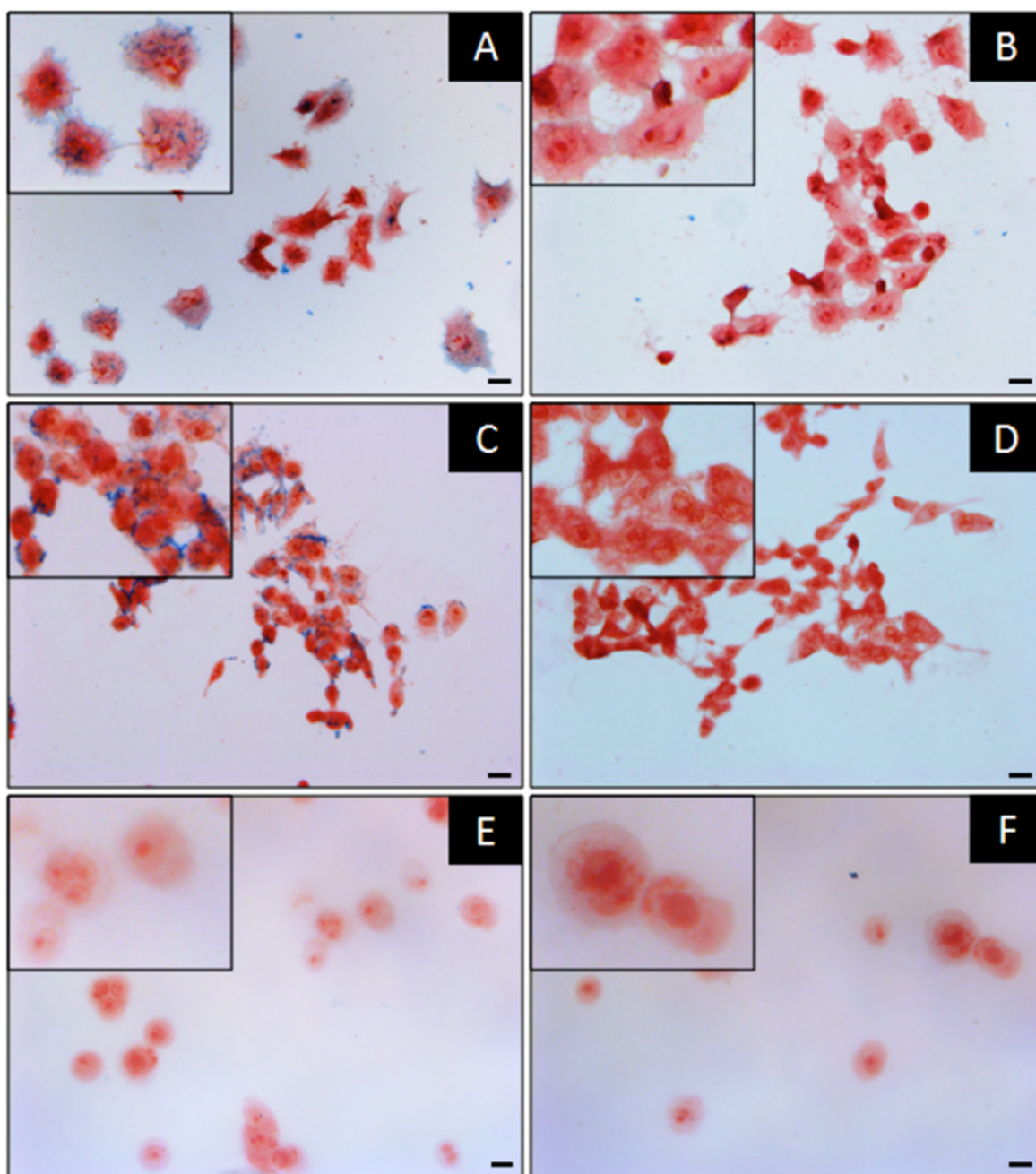
**Figure 3.** Prussian blue staining of Panc-1 cells incubated with (a) MNP-antiCD44 and (b) MNPs, MDA-MB-231 cells incubated with (c) MNP-antiCD44 and (d) MNPs, and MCF-10A  incubated with (e) MNP-antiCD44 and (f) MNP (scale bar = 20 $\mu$m).

are seen in the periphery of the cells. The MNPs were mainly found as aggregates of variable size. Small aggregates were seen adjacent to the outer side of the cell membrane, but they were never found inside the cell cytoplasm. On the contrary, the MNP-antiCD44 (figure 4(b)) showed a more dispersed aspect. The majority of particles were found as isolated MNPs (21-23 nm in diameter) near or in direct contact with the outer side of the cell membrane, suggesting an even distribution of the interacting domains (figure 4(b), and inset). MNP-antiCD44 was also found to be incorporated into clathrin-coated vesicles in a few cases (figure 4(b), insets), which did not happen with control MNPs (figure 4(a)). DLS

measurements in cell culture media confirmed partial aggregation of the MNPs without antibodies in comparison with the MNP-antiCD44 (supporting information, figure S3).

These results are fully consistent with the idea that the presence of antiCD44 antibodies on the surface of the MNPs directs nanoparticles towards specific interaction with CD44 in the outer membrane of overexpressing cell lines. This interaction was essentially absent in the incubation with control MNPs that lacked the antibody, as expected under the low-temperature conditions used to minimize the energy-dependent unspecific endocytosis processes. In some cases, we found MNP-antiCD44 particles inside what seem to be
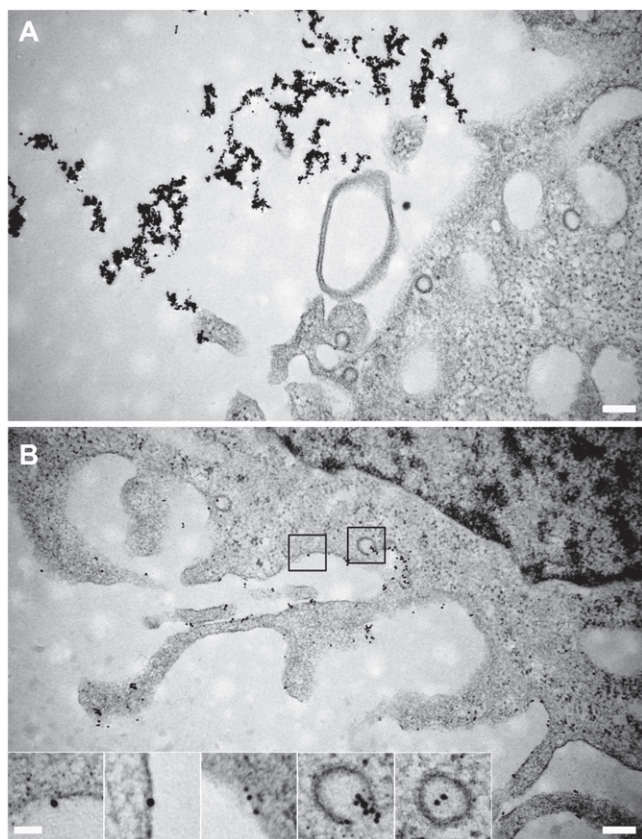
**Figure 4.** Electron microscopy images of thin sections of cells incubated with MNPs. (a) MDA-MB-231 cells incubated with control MNPs. The particles are aggregated into high-density groups in the cell periphery. (b) Cells incubated with MNP-antiCD44. The MNPs are dispersed as 12–14 nm high-density particles very near or in contact with the outer side of the cell membrane (insets, left). The MNPs were also seen in vesicles that might be associated to clathrin coating (insets, right). The insets show representative cases of MNPs interacting with plasmatic membrane (left) or incorporated into vesicles (right). The scale bar represents 200 nm (50 nm in the insets).

clathrin-coated vesicles inside the cell cytoplasm. Clathrin is known to facilitate the receptor-mediated endocytosis of a variety of ligands, although participation of CD44 in receptor-mediated endocytosis is not always clathrin-dependent [41, 42]. Our results indicate that this pathway might also be involved in MNP specific internalization.

*3.3.3. Downregulation of CD44 expression.* To further confirm the specificity of the binding of MNP-antiCD44 to cells, CD44 was downregulated using siRNA. The control experiments using MNP without antiCD44 Ab in combination with siRNA control or CD44 siRNA did not show significant cellular internalization (figures 5, (b)). As expected, MNP-antiCD44 were clearly internalized by MDA-MB-231 cells transfected with control siRNA (figure 5(c)). On the other hand, knockdown of CD44 expression inhibited the binding and consequent uptake of MNPs functionalized with CD44 antibodies, confirming targeting specificity

(figure 5(d)). These results validate the successful functionalization of MNPs with CD44 antibodies.

*3.4. In vitro efficacy of MNP-GEM-antiCD44 in CD44-positive cancer cell lines*

Finally, the ability of the MNP-GEM and MNP-GEM-antiCD44 to deliver GEM and induce cell death compared with free GEM was examined on Panc-1, MDA-MB231 and MCF-10A by the Alamar Blue assay. The incubation with the different formulations was done at 4 °C in order to avoid the non-specific endocytosis processes of the MNPs. Cells were then washed with PBS and incubated for 3 days at 37 °C. Significant differences between the MNP-GEM and MNP-GEM-antiCD44 were evident 3 days after the drug treatment (figure 6). Greater antiproliferative activity was observed in CD44-positive cancer cells (Panc-1 and MDA-MB231) for MNP-GEM-antiCD44 (4 $\mu$M of GEM) compared with MNP-GEM (4 $\mu$M of GEM ($^{**}P < 0.01$ and $^{*}P < 0.05$) (figures 6(a) and (b)). Also, significant differences were observed 3 days after the drug treatment between the MNP-GEM-antiCD44 and free-drug doses (0.4 and 1 $\mu$M of GEM) ($^{*}P < 0.05$). No significant differences between the MNP-GEM-antiCD44 (4 $\mu$M of GEM) and the higher free-drug dose (4 $\mu$M of GEM) were observed after 3 days of treatment. In the case of the non-tumorigenic CD44-negative cell line (MCF-10A), no antiproliferative activity was observe with both formulation (MNP-GEM-antiCD44 and MNP-GEM) in comparison with the free drug . This result confirms the target-specific intracellular GEM delivery capacity of multi-functionalized MNPs with GEM and antiCD44 antibodies and confirms that the drug release mechanism only occurs inside the cell (figure 6).

## 4. Conclusions

We have developed a novel multifunctionalized MNP for selective targeting of CD44-positive cancer cells. *In vitro* studies demonstrated that antiCD44 functionalized MNPs bind specifically to the CD44 surface receptor that is overexpressed on pancreatic and breast cancer cells. The selective targeting mechanism was confirmed by ultrastructural characterization and downregulation of CD44 expression. Finally, we show the potential of multifunctionalized MNPs for targeted drug delivery towards pancreatic cancer cells. As a proof of our controlled drug release system, covalently immobilized GEM on MNPs shows a selective and rapid release in intracellular conditions. *In vitro*, the delivery of GEM to CD44-positive cancer cells overexpressing the CD44 receptor increased when a multifunctional targeting system is used. The antitumoural efficacy of the multifunctional formulation is significantly improved compared with free-drug delivery and with the delivery using non-targeted nanoparticles. These results indicated that the novel nanoplatform developed here possesses great potential to be applied in targeted cancer therapy. This study contributes to the growing knowledge of specifically targeting cancer cells using
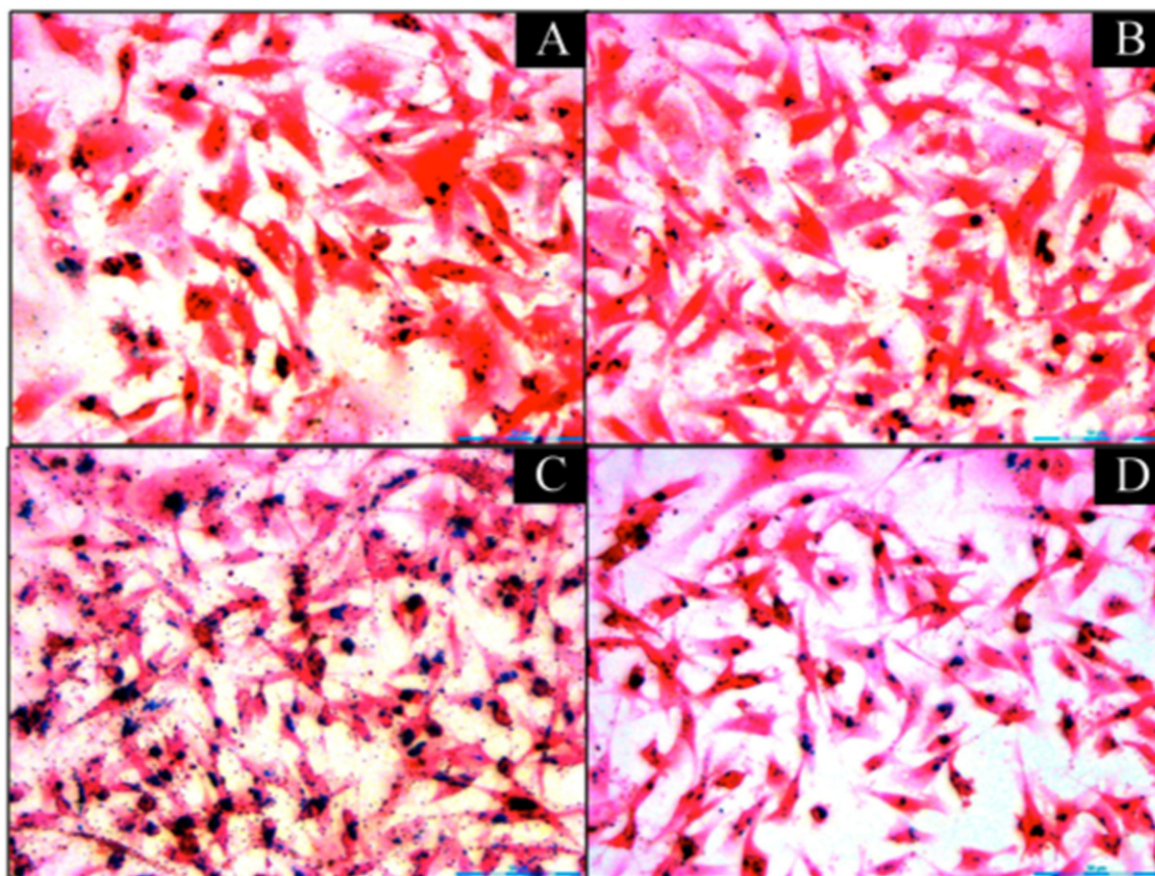
**Figure 5.** Prussian blue staining of MDA-MB-231 cells incubated with (a) MNP + Control siRNA; (b) MNP + CD44 siRNA; (c) MNP-antiCD44 + Control siRNA and (d) MNP-antiCD44 + CD44 siRNA. (Scale bar = 50 $\mu$m).
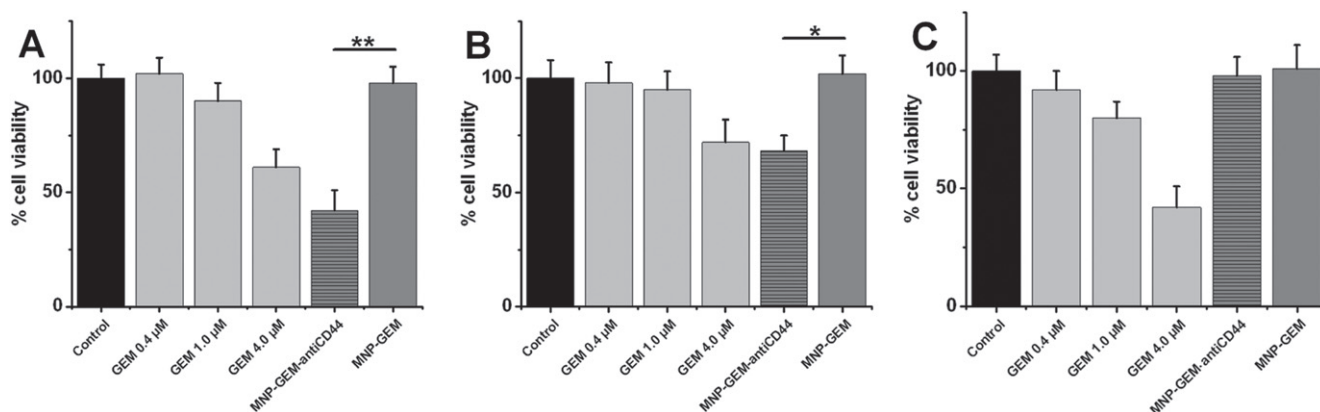


**Figure 6.** Viability of (a) Panc-1, (b) MDA-MB231 and (c) MCF-10A cells untreated (control) and treated with free GEM (0.4, 1 and 4 $\mu$M), MNP-GEM-antiCD44 (4 $\mu$M GEM) and MNP-GEM (4 $\mu$M GEM).

multifunctionalized MNPs. In the long term, it is expected that these advances could be translated into the clinical setting and therefore result in improved and more targeted therapies for cancer.

## References

[1] Couvreur P 2013 *Adv. Drug Deliv. Rev.* **65** 21–3
[2] Mahmoudi M, Sant S, Wang B, Laurent S and Sen T 2011 *Adv. Drug Deliv. Rev.* **63** 24–46

[3] Cortajarena A L, Ortega D, Ocampo S M, Gonzalez-garcía A, Couleaud P, Miranda R, Belda-Iniesta C and Ayuso-Sacino A 2014 *Nanobiomedicine* **1** 1–20

[4] Jabr-Milane L S, van Vlerken L E, Yadav S and Amiji M M 2008 *Cancer Treat. Rev.* **34** 592–602

[5] Cho K, Wang X, Nie S, Chen Z G and Shin D M 2008 *Clin. Cancer Res.* **14** 1310–6

[6] Veiseh O, Gunn J W and Zhang M 2010 *Adv. Drug Deliv. Rev.* **62** 284–304

[7] Ravichandran R 2009 *NanoBiotechnology* **5** 17–33

[8] Naahidi S, Jafari M, Edalat F, Raymond K, Khademhosseini A and Chen P 2013 *J. Control. Release* **166** 182–94

[9] Krishnan K M 2010 *IEEE Trans. Magn.* **46** 2523–58

[10] Mejías R *et al* 2011 *Biomaterials* **32** 2938–52

[11] Salas G, Casado C, Teran F J, Miranda R, Serna C J and Morales M D P 2012 *J. Mater. Chem.* **22** 21065–75

[12] Pesarrodona M *et al* 2014 *Int. J. Pharm.* **473** 286–95

[13] Wang L *et al* 2012 *Biomaterials* **33** 5107–14

[14] Lee E, Hong Y, Choi J, Haam S, Suh J S, Huh Y M and Yang J 2012 *Nanotechnology* **23** 465101–8

[15] Baccelli I *et al* 2013 *Nat. Biotechnol.* **31** 539–44

[16] Sheridan C, Kishimoto H, Fuchs R K, Mehrotra S, Bhat-Nakshatri P, Turner C H, Goulet R Jr, Badve S and Nakshatri H 2006 *Breast Cancer Res.* **8** R59

[17] Ponta H, Sherman L and Herrlich P A 2003 *Nat. Rev. Mol. Cell Biol.* **4** 33–45

[18] Zoller M 2011 *Nat. Rev. Cancer* **11** 254–67

[19] Al-Hajj M, Wicha M S, Benito-Hernandez A, Morrison S J and Clarke M F 2003 *Proc. Natl Acad. Sci. USA* **100** 3983–8

[20] Shipitsin M *et al* 2007 *Cancer Cell* **11** 259–73

[21] Reya T, Morrison S J, Clarke M F and Weissman I L 2001 *Nature* **414** 105–11

[22] Peer D, Karp J M, Hong S, Farokhzad O C, Margalit R and Langer R 2007 *Nat. Nanotechnol.* **2** 751–60

[23] Goodison S, Urquidi V and Tarin D 1999 *Mol. Pathol.* **52** 189–96

[24] Gee K, Kryworuchko M and Kumar A 2004 *Arch. Immunol. Ther. Exp.* **52** 13–26

[25] Cardoso M M, Peça I N and Roque A C A 2012 *Curr. Med. Chem.* **19** 3103–27

[26] Dawidczyk C M, Kim C, Park J H, Russell L M, Lee K H, Pomper M G and Searson P C 2014 *J. Control. Release* **187** 133–44

[27] Yin T, Wei H, Gou S, Shi P, Yang Z, Zhao G and Wang C 2011 *Int. J. Mol. Sci.* **12** 1595–604

[28] Asuthkar S, Stepanova V, Lebedeva T, Holterman A L, Estes N, Cines D B, Rao J S and Gondi C S 2013 *Mol. Biol. Cell.* **24** 2620–32

[29] Ricardo S, Vieira A F, Gerhard R, Leitão D, Pinto R, Cameselle-Teijeiro J F, Milanezi F, Schmitt F and Paredes J 2011 *J. Clin. Pathol.* **64** 937–46

[30] Dreaden E C, Morton S W, Shopsowitz K E, Choi J, Deng Z J, Cho N J and Hammond P T 2014 *ACS Nano* **8** 8374–82

[31] Latorre A, Couleaud P, Aires A, Cortajarena A L and Somoza A 2014 *Eur. J. Med. Chem.* **82** 355–62

[32] Marciello M, Connord V, Veintemillas-Verdaguer S, Vergés M A, Carrey J, Respaud M, Serna C J and Morales M P 2013 *J. Mater. Chem.* B **1** 5995–6004

[33] Creighton T E 1989 Disulfide bonds between cysteine residues *Protein Structure: A Practical Approach* ed T E Creighton (Oxford: IRL Press at Oxford University Press) pp 155–67

[34] Bradford M M 1976 *Anal. Biochem.* **72** 248–54

[35] Chichón F J *et al* 2012 *J. Struct. Biol.* **177** 202–11

[36] Saito G, Swanson J and Lee K 2003 *Adv. Drug Deliv. Rev.* **55** 199–215

[37] Traut R R, Bollen A, Sun T T, Hershey J W, Sundberg J and Pierce L R 1973 *Biochemistry* **12** 3266–73

[38] Puertas S, Moros M, Fernández-Pacheco R, Ibarra M R, Grazú V and de la Fuente J M 2010 *J. Phys. D. Appl. Phys.* **43** 474012–9

[39] Hadjidemetriou M, Al-Ahmady Z, Mazza M, Collins R F, Dawson K and Kostarelos K 2015 *ACS Nano* **9** 8142–56

[40] Hermanson G T 2008 *Bioconjugate Techniques* 2nd edn ed Greg T Hermanson (New York: Academic) pp 793–5

[41] Hirst J and Robinson M S 1998 *Biochim. Biophys. Acta-Mol. Cell Res.* **1404** 173–93

[42] Kirchhausen T 2000 *Annu. Rev. Biochem.* **69** 699–727